

# Egyptian Geoid using Ultra High-Degree Tailored Geopotential Model

Hussein A. ABD-ELMOTAAL, Egypt

**Keywords:** tailored geopotential models, harmonic analysis, window technique, Egypt, geoid determination.

## SUMMARY

In the framework of the remove-restore technique, the residual field should be unbiased and have a small variance. Hence, an ultra high-degree (complete to degree and order 2160) reference geopotential model tailored to Egypt is developed within this investigation. The local and global data sets, in terms of isostatic gravity anomalies, are merged and used to estimate the harmonic coefficients of the ultra high-degree tailored reference model by an FFT technique using an iterative process to enhance the accuracy of the obtained harmonic coefficients and to minimize the residual field (Abd-Elmotaal, 2004). This tailored geopotential model has then been used to compute a gravimetric geoid for Egypt in the framework of the remove-restore technique. The window technique (Abd-Elmotaal and Kührtreiber, 2003) has been used to avoid the double consideration of some of the topographic-isostatic masses in the neighbourhood of the computational point. The commonly used Airy-Heiskanen isostatic hypothesis is applied. For the sake of comparison, the EGM2008 global geopotential model has also been used. The gravimetric geoids are computed for Egypt using Stokes' integral in the frequency domain by 1-D FFT technique. The computed geoids are scaled/fitted to the GPS/levelling derived geoid. The results show that the tailored ultra high-degree geopotential model created in this investigation gives better residual gravity anomalies (unbiased and have smaller variance) as well as better geoid accuracy. The variance of the residual gravity anomalies has dropped by about 35%. The external accuracy of the fitted geoid has improved by about 20 %.

# Egyptian Geoid using Ultra High-Degree Tailored Geopotential Model

Hussein A. ABD-ELMOTAAL, Egypt

## 1. INTRODUCTION

The quality of the reference geopotential model used in the framework of the remove-restore technique plays a great role in estimating the accuracy of the computed geoid. In other words, if the residual field is biased and has a high variance, then using such a biased/high variance field in the geoid computation process gives less accurate interpolated quantities, and hence worse geoid fitting to the GPS/levelling derived geoid. Practical studies so far have proved that none of the existing reference geopotential models fit the Egyptian gravity field to the desired extent (see, e.g., Abd-Elmotaal, 2009). Thus, one of the aims of this investigation is to have a smoothed gravity anomalies field so that it is unbiased and has a significantly small variance by using an ultra high-degree (complete to degree and order 2160) tailored reference geopotential model. Such a tailored geopotential model is then used to compute a gravimetric geoid for Egypt in the framework of the remove-restore technique.

The used data sets are described. The window technique (Abd-Elmotaal and Kühtreiber, 2003) within the remove-restore technique has been outlined. The local gravity anomalies for the Egyptian data window are gridded, after removing the effect of the topographic-isostatic masses for the data window as well as the effect of EGM2008 from  $n = 361$  to  $n = 2160$ , in  $30' \times 30'$  grid using kriging interpolation technique. The local gridded data are merged with the global  $30' \times 30'$  gravity anomalies, computed using EGM2008 till  $N = 360$  after removing the effect of the global topographic-isostatic masses using SRTM  $30' \times 30'$  DHM, to establish the data set for computing the tailored geopotential models. The merged  $30' \times 30'$  global field has been then used to estimate the harmonic coefficients of the tailored reference model by an FFT technique (Abd-Elmotaal, 2004) till degree and order 360. The higher coefficients (from  $n = 361$  to  $n = 2160$ ) of EGM2008 has then been restored generating the ultra high-degree tailored geopotential model complete to degree and order 2160. The generated tailored geopotential model has been used, in the framework of the remove-restore technique using the window technique, to compute a gravimetric geoid for Egypt. The EGM2008 geopotential model, complete to degree and order 2160, has also been used to compute a gravimetric geoid for Egypt for comparison purposes. A comprehensive comparison between using the developed tailored geopotential model and the EGM2008 geopotential model in terms of the reduced anomalies and computed geoids has been carried out.

It should be noted that many scholars have tried to compute tailored geopotential models to best suit their specific areas of interest. The reader may refer, e.g., to (Kearsley and Forsberg, 1990; Wenzel, 1998; Abd-Elmotaal, 2007; Abd-Elmotaal et al., 2013).

## 2. THE DATA

### 2.1. Local Egyptian Free-Air Gravity Anomalies

All currently available sea and land free-air gravity anomalies for Egypt and neighbouring countries have been merged. A scheme for gross-error detection has been carried out. **The gravity data set for Egypt refer to the International Gravity Standardization Net 1971 (IGSN-71). The WGS84 coordinate system is utilized.**

Figure 1 shows the distribution of the free-air gravity anomalies for Egypt used for the current investigation. The distribution of the free-air gravity anomaly stations on land is very poor. Many areas are empty. The distribution of the data points at the Red Sea is better than that at the Mediterranean Sea.

A total number of 102418 gravity values are available. The free-air gravity anomalies range between  $-210.60$  mgal and  $314.99$  mgal with an average of  $-27.58$  mgal and a standard deviation of about  $50.65$  mgal. Highest values are in sea region.

### 2.2. Digital Height Models

For the terrain reduction computation, a set of fine and coarse Digital Height Models DHM's is needed. The fine EGH13S03  $3'' \times 3''$  and the coarse EGH13S30  $30'' \times 30''$  DHM's (Abd-Elmotaal and Ashry, 2013) are used for the current investigation. They cover the window  $19^\circ \leq \phi \leq 35^\circ$ ,  $22^\circ \leq \lambda \leq 40^\circ$ . Figure 2 illustrates the EGH13S03  $3'' \times 3''$  fine DHM. **It should be mentioned that the Helmert orthometric height system is used in Egypt.**

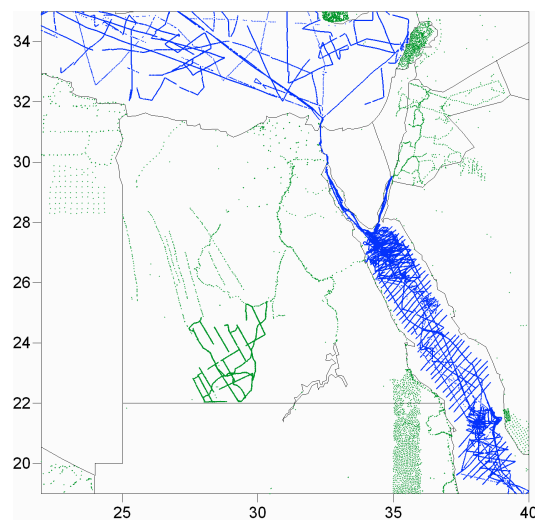


Figure 1: Distribution of the local Egyptian free-air gravity anomalies.

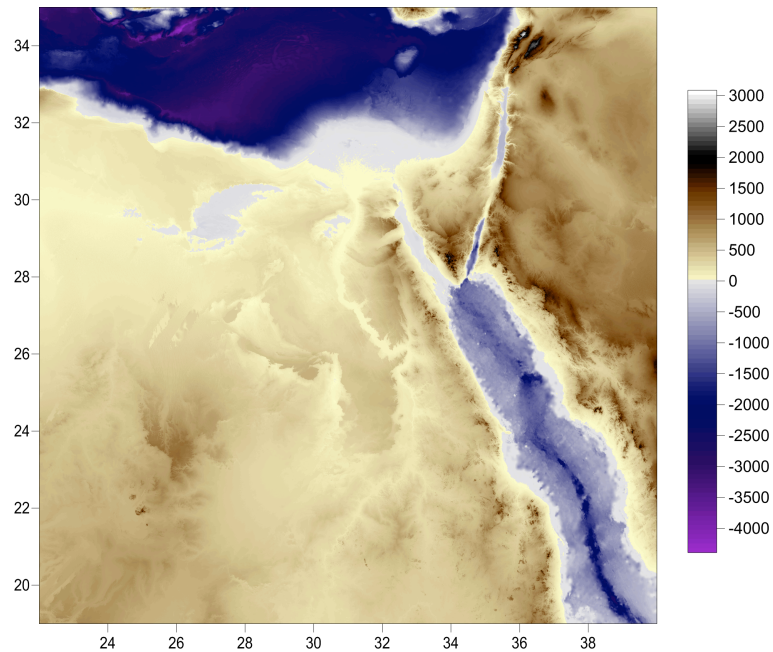


Figure 2: The 3"  $\times$  3" EGH13S03 Digital Height Model (after Abd-Elmotaal and Ashry, 2013). Values are in meters.

### 2.3. GPS Stations

The distribution of the most reliable/available GPS stations with known orthometric height is shown in Fig. 3. The distribution is fairly good, but the total number of the GPS stations is too small in relation to Egypt's surface area.

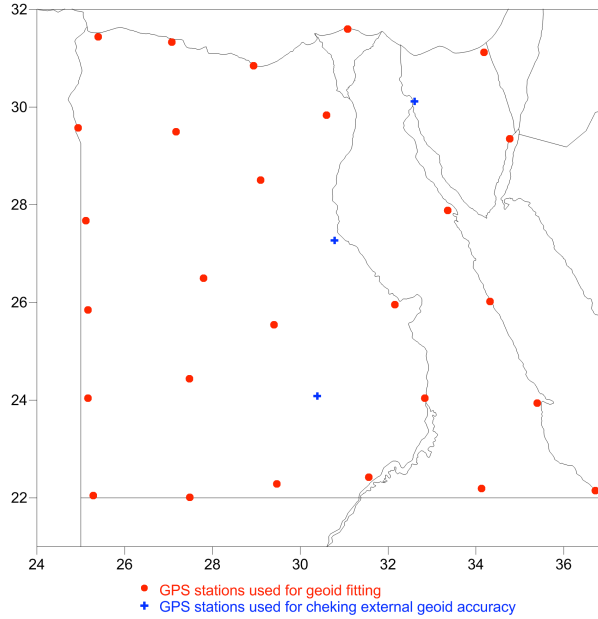


Figure 3: Distribution of the GPS stations with known orthometric height in Egypt.

### 3. THE WINDOW TECHNIQUE

Within the well-known remove-restore technique (Forsberg, 1984), the effect of the topographic-isostatic masses is removed from the source gravitational data and then restored to the resulting geoidal heights. For example, in the case of gravity data, the reduced gravity anomalies  $\Delta g_{red}$  in the framework of the remove-restore technique is computed by

$$\Delta g_{red} = \Delta g_F - \Delta g_{TC} - \Delta g_{GM}, \quad (1)$$

where  $\Delta g_F$  stands for the free-air anomalies,  $\Delta g_{TC}$  is the terrain reduction due to the topographic-isostatic masses, and  $\Delta g_{GM}$  is the effect of the reference field (global geopotential model) on the gravity anomalies. Thus the final computed geoid  $N$  within the remove-restore technique can be expressed by:

$$N = N_{GM} + N_{\Delta g} + N_{TC}, \quad (2)$$

where  $N_{GM}$  gives the contribution of the reference field,  $N_{\Delta g}$  gives the contribution of the reduced gravity anomalies, and  $N_{TC}$  gives the contribution of the topography and its compensation (the indirect effect).

The traditional way of removing the effect of the topographic-isostatic masses faces a problem. A part of the influence of the topographic-isostatic masses is removed twice as it is already included in the global reference field. This leads to some double consideration of that part of the topographic-isostatic masses. Figure 4 shows schematically the traditional gravity reduction for the effect of the topographic-isostatic masses. The short-wavelength

part depending on the topographic-isostatic masses is computed for a point  $P$  for the masses inside the circle (say till 167 km around the computational point  $P$ ; denoted by  $TC$  in Fig. 4). Removing the effect of the long-wavelength part by a global earth's gravitational reference field normally implies removing the influence of the global topographic-isostatic masses (shown as the full rectangle in Fig. 4). The double consideration of the topographic-isostatic masses inside the circle (double hatched) is then seen.

A possible way to overcome this difficulty in computing geoidal heights from topographic-isostatic reduced gravity anomalies is to adapt the used reference field due to the effect of the topographic-isostatic masses for a fixed local data window (denoted by the small rectangle in Fig. 5). Figure 5 shows the advantage of the window remove-restore technique.

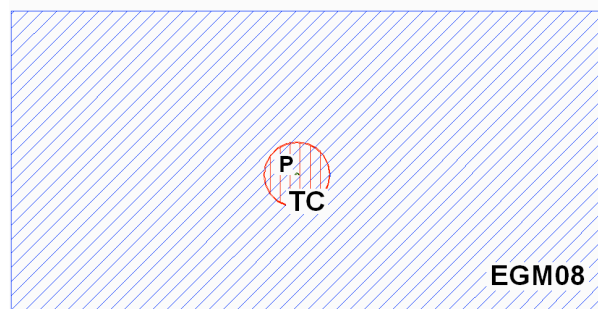


Figure 4: The traditional remove-restore technique.

Let us concentrate on the influence of the topographic-isostatic masses in the reduction process. Consider a measurement at point  $P$ , the short-wavelength part depending on the topographic-isostatic masses is now computed by using the masses of the whole data area (the small rectangle in Fig. 5). The adapted reference field is created by subtracting the effect of the topographic-isostatic masses of the data window, in terms of potential coefficients, from the reference field coefficients (adapted reference field is then represented by the area of the big rectangle, representing the globe, minus the area of the small rectangle, representing the local data area; cf. Fig. 5). Thus, removing the long-wavelength part by using this adapted reference field does not lead to a double consideration of a part of the topographic-isostatic masses (there is no double hatched area in Fig. 5).

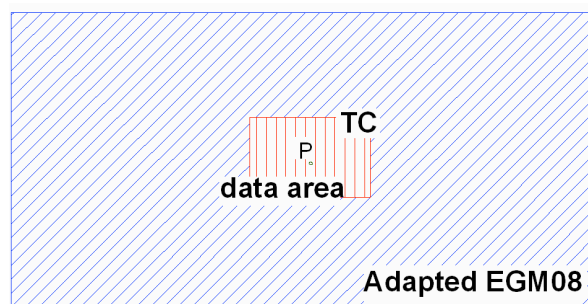


Figure 5: The window remove-restore technique.

The remove step of the window remove-restore technique can then mathematically be written as

$$\Delta g_{red} = \Delta g_F - \Delta g_{TC\ win} - \Delta g_{GM\ Adapt} , \quad (3)$$

where  $\Delta g_{GM\ Adapt}$  is the contribution of the adapted reference field and  $\Delta g_{TC\ win}$  stands for the terrain reduction of the topographic-isostatic masses for a fixed data window. The restore step of the window remove-restore technique can be written as

$$N = N_{GM\ Adapt} + N_{\Delta g} + N_{TC\ win} , \quad (4)$$

where  $N_{GM\ Adapt}$  gives the contribution of the adapted reference field and  $N_{TC\ win}$  gives the contribution of the topography and its compensation (the indirect effect) for the same fixed data window as used for the remove step.

#### 4. HARMONIC ANALYSIS OF THE TOPOGRAPHIC-ISOSTATIC POTENTIAL

The harmonic coefficients of the topography and its isostatic compensation as well as the harmonic series expansion of the topographic-isostatic potential can be expressed by (Abd-Elmotaal and Kühtreiber, 2003, pp. 78–79):

$$T_{II}(P) = \frac{GM}{r_P} \sum_{n=0}^{\infty} \left( \frac{R}{r_P} \right)^n \sum_{m=-n}^n \bar{T}_{nm} \bar{R}_{nm}(P) , \quad (5)$$

where

$$\begin{aligned} \bar{T}_{nm} = & \frac{R^3}{M(2n+1)(n+3)} \iint_{\sigma} \left\{ \delta\rho_Q \left[ \left( 1 + \frac{H_Q}{R} \right)^{n+3} - 1 \right] + \right. \\ & \left. + \delta\rho_Q \left( 1 - \frac{T_o}{R} \right)^{n+3} \left[ \left( 1 - \frac{t_Q}{R - T_o} \right)^{n+3} - 1 \right] \right\} \bar{R}_{nm}(Q) d\sigma_Q , \end{aligned} \quad (6)$$

where  $T_o$  is the normal crustal thickness,  $H$  is the topographic height,  $t$  is the compensating root/antiroot and  $M$  denotes the mass of the earth, given by

$$M \cong \frac{4\pi R^3}{3} \rho_M , \quad (7)$$

where  $\rho_M$  denotes the mean earth's density (Sünkel, 1985)

$$\rho_M \cong 5.517 \text{ g/cm}^3 .$$

For the practical determination of the harmonic coefficients of the topographic-isostatic potential, (6) may be written as

$$\begin{aligned} \bar{T}_{nm} = & \frac{3\Delta\phi\Delta\lambda}{4\pi\rho_M(2n+1)(n+3)} \sum_i^\phi \sum_j^\lambda \left\{ \rho_{ij} \left[ \left( 1 + \frac{H_{ij}}{R} \right)^{n+3} - 1 \right] + \right. \\ & \left. + \Delta\rho_{ij} \left( 1 - \frac{T_o}{R} \right)^{n+3} \left[ \left( 1 - \frac{t_{ij}}{R-T_o} \right)^{n+3} - 1 \right] \right\} \begin{Bmatrix} \cos m\lambda_j \\ \sin m\lambda_j \end{Bmatrix} \bar{P}_{nm}(\cos\theta_i) \cos\phi_i, \end{aligned} \quad (8)$$

where  $\sum$  denotes the summation along  $\phi$  and  $\lambda$ ,  $\Delta\phi$  and  $\Delta\lambda$  are the grid sizes of the used Digital Height Model in the latitude and the longitude directions, respectively,  $\rho$  is given by

$$\begin{aligned} \rho &= \rho_o & \text{for } H \geq 0, \\ \rho &= \rho_o - \rho_w & \text{for } H < 0, \end{aligned} \quad (9)$$

where  $\rho_o$  denotes the density of the topography and  $\rho_w$  is the density of sea water. The density anomaly  $\Delta\rho$  is given by

$$\Delta\rho = \rho_1 - \rho_o, \quad (10)$$

where  $\rho_1$  is the density of the upper mantle.

In case of the Airy-Heiskanen isostatic model, the thickness of the root/antiroot  $t$  is determined by applying the principle of mass balance, which can be written in the spherical approximation as (Rummel et al., 1988, p. 3)

$$\rho_o R^3 \left[ \left( 1 + \frac{H}{R} \right)^3 - 1 \right] = (\rho_1 - \rho_o) (R - T_o)^3 \left[ 1 - \left( 1 - \frac{t}{R - T_o} \right)^3 \right]. \quad (11)$$

This condition can be written for the thickness of the root/antiroot  $t$  as follows:

$$\frac{t}{R - T_o} = 1 - \left\{ 1 - \frac{\rho}{\rho_1 - \rho_o} \left( 1 - \frac{T_o}{R} \right)^{-3} \left[ \left( 1 + \frac{H}{R} \right)^3 - 1 \right] \right\}^{\frac{1}{3}}, \quad (12)$$

where  $\rho$  is given by (9).

## 5. CREATING THE TAILORED GEOPOTENTIAL MODEL FOR EGYPT

### 5.1. Methodology

As we mentioned above, the ultra high-degree tailored geopotential model is going to be created in the framework of the window technique. Let us re-write the remove expression (3) of the window technique as follows:

$$\begin{aligned} \Delta g_{red} &= \Delta g_F - \Delta g_{TC\ win} - \Delta g_{GM\ Adapt} \\ &= \Delta g_F - \Delta g_{TC\ win} - (\Delta g_{GM} - \Delta g_h), \end{aligned} \quad (13)$$

where  $\Delta g_h$  stands for the contribution of the harmonic coefficients, computed using (8), of the topographic-isostatic masses of the data window. The contribution of the global geopotential model  $\Delta g_{GM}$  (if the maximum available degree of the model is, e.g., 2160) can be written as

$$\Delta g_{GM} = \Delta g_{GM}|_{0 \leq n \leq 360} + \Delta g_{GM}|_{361 \leq n \leq 2160} . \quad (14)$$

Thus (13) can finally be written as

$$\Delta g_{red} = \Delta g_F - \Delta g_{TCwin} - \Delta g_{GM}|_{0 \leq n \leq 360} - \Delta g_{GM}|_{361 \leq n \leq 2160} + \Delta g_h . \quad (15)$$

If we aim to have, theoretically, zero reduced anomalies by tailoring the geopotential model, then the left hand-side of (15) is put to zero. If we keep the higher harmonics of the tailored geopotential model to their values as of the existing global model (e.g., EGM2008), thus we can compute the gravity anomalies referring to the tailored geopotential model  $\Delta g_{GM_T}$  as:

$$\Delta g_{GM_T}|_{0 \leq n \leq 360} = \Delta g_F - \Delta g_{TCwin} - \Delta g_{GM}|_{361 \leq n \leq 2160} + \Delta g_h . \quad (16)$$

## 5.2. Preparing the Gravity Anomalies

The SRTM 30' × 30' global DHM (Farr et al., 2007) has been used to compute the harmonic coefficients of the global topographic-isostatic masses  $T_{TI}$  using (8) till  $n = 360$ . Figure 6 shows the SRTM 30' × 30' global DHM. The heights range between -8756 m and 5719 m with an average of about -1892 m and standard deviation of 2638 m.

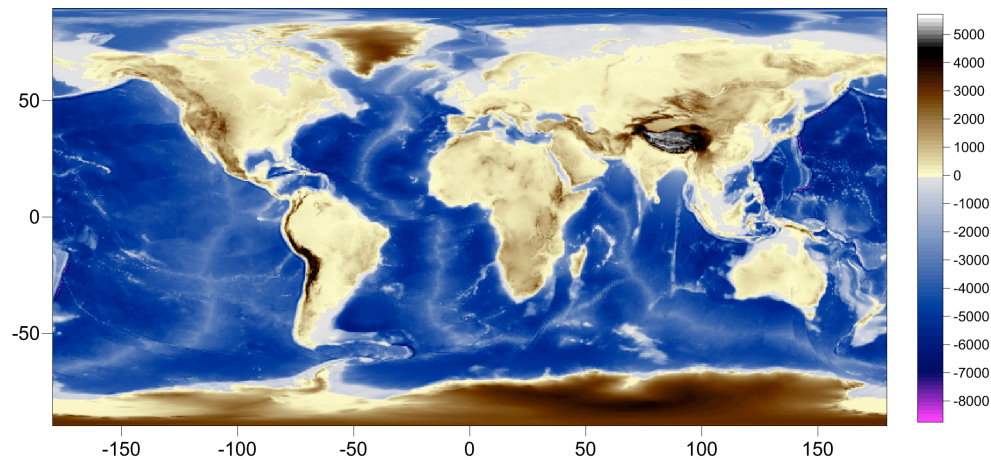


Figure 6: SRTM 30' × 30' global DHM. Values are in meters.

The global isostatic harmonic coefficients are created by subtracting the harmonic coefficients of the global topographic-isostatic masses  $T_{TI}$  from those of the EGM2008 model (Pavlis et al., 2008, 2012). These global isostatic harmonic coefficients, till  $n = 360$ , are used to generate a global **isostatic** 30' × 30' field of isostatic anomalies.

The local Egyptian data have been **isostatically reduced** according to (16). It should be noted that by subtracting the effect of EGM2008 (from  $n = 361$  to  $n = 2160$ ) from the measured free-air gravity anomalies, we assumed that the reduced anomalies contain only the lower harmonics till  $n = 360$  (of course the measured gravity contains the contribution of even higher degrees than 2160, but we neglect them in the computation of the tailored model).

The local Egyptian reduced anomalies have been interpolated in  $30' \times 30'$  grid using the kriging interpolation technique. Figure 7 shows the local Egyptian  $30' \times 30'$  interpolated anomalies.

The local Egyptian  $30' \times 30'$  interpolated **isostatically reduced** gravity anomalies have been merged with the created  $30' \times 30'$  global isostatic gravity anomalies forming the data set for computing the tailored geopotential model for Egypt. Figure 8 shows that merged field.

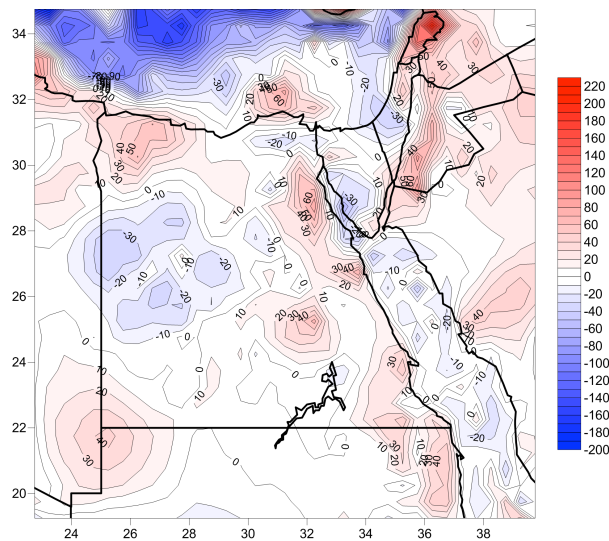


Figure 7: The local Egyptian  $30' \times 30'$  interpolated **isostatically reduced** gravity anomalies. Contour interval: 10 mgal.

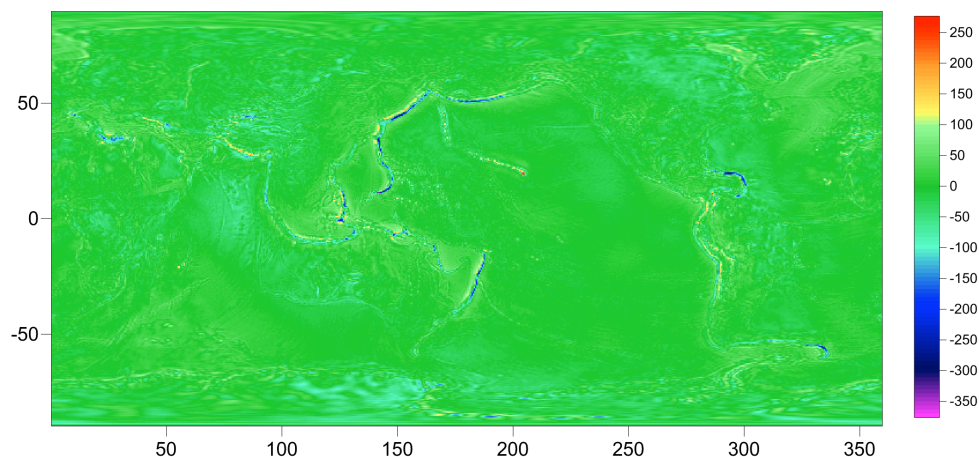


Figure 8: The **reduced** global  $30' \times 30'$  merged field including Egyptian gravity anomalies. Values are in mgal.

Table 1 illustrates the statistics of the used three gravity anomalies fields. The statistics show that merging the Egyptian gravity anomalies data set has a minor effect on the global gravity field.

Table 1: Statistics of the used three gravity anomalies fields

gravity anomalies type	statistical parameters			
	min.	max.	average	st. dev.
	mgal	mgal	mgal	mgal
Global isostatic (EGM2008)	-337.0	273.2	-0.85	27.2
Local isostatic (Egypt)	-190.0	202.0	0.25	36.7
Merged isostatic (EGM2008 + Egypt)	-337.0	273.2	-0.86	27.3

### 5.3. Harmonic Analysis of a Global Field Using FFT

Let us consider an analytical function  $f(\theta, \lambda)$  defined on the unit sphere ( $0 \leq \theta \leq \pi$  and  $0 \leq \lambda \leq 2\pi$ ). Expand  $f(\theta, \lambda)$  in series of surface spherical harmonics

$$f(\theta, \lambda) = \sum_{n=0}^{\infty} \sum_{m=0}^n (\bar{C}_{nm} \cos m\lambda + \bar{S}_{nm} \sin m\lambda) \bar{P}_{nm}(\cos \theta), \quad (17)$$

where  $\bar{C}_{nm}$  and  $\bar{S}_{nm}$  are the fully normalized harmonic coefficients and  $\bar{P}_{nm}(\cos \theta)$  refers to the fully normalized associated Legendre function.

It is well known that the fully normalized harmonic coefficients are orthogonal. Consequently, the fully normalized harmonic coefficients  $\bar{C}_{nm}$  and  $\bar{S}_{nm}$  can be given by (Heiskanen and Moritz, 1967, p. 31)

$$\begin{aligned} \bar{C}_{nm} &= \frac{1}{4\pi} \iint_{\sigma} f(\theta, \lambda) \bar{P}_{nm}(\cos \theta) \cos m\lambda d\sigma, \\ \bar{S}_{nm} &= \frac{1}{4\pi} \iint_{\sigma} f(\theta, \lambda) \bar{P}_{nm}(\cos \theta) \sin m\lambda d\sigma. \end{aligned} \quad (18)$$

In fact, (18) cannot be used in practice to compute the harmonic coefficients simply because the analytical function  $f(\theta, \lambda)$  is generally unavailable. Only a finite set of noisy measurements  $f(\theta_i, \lambda_j)$ , covering the whole sphere, might be available. Discretizing (18) on an equal angular grid covering the whole sphere gives the following quadratures formula

$$\begin{aligned}\hat{C}_{nm} &= \frac{1}{4\pi} \sum_{i=0}^{N-1} \sum_{j=0}^{2N-1} f(\theta_i, \lambda_j) \bar{P}_{nm}(\cos \theta_i) \cos m\lambda_j \Delta_{ij}, \\ \hat{S}_{nm} &= \frac{1}{4\pi} \sum_{i=0}^{N-1} \sum_{j=0}^{2N-1} f(\theta_i, \lambda_j) \bar{P}_{nm}(\cos \theta_i) \sin m\lambda_j \Delta_{ij},\end{aligned}\tag{19}$$

where  $\hat{C}_{nm}$  and  $\hat{S}_{nm}$  are the estimate of  $\bar{C}_{nm}$  and  $\bar{S}_{nm}$ , respectively,  $\Delta_{ij}$  indicates the segment area and  $N$  is the number of grids in the latitude direction. Expression (19) is used to compute the harmonic coefficients if the available data field is represented by a set of point values  $f(\theta_i, \lambda_j)$ . It should be noted that (19) is usually only an approximation due to the discretization effect of  $f(\theta, \lambda)$ .

If all  $\bar{C}_{nm}$  and  $\bar{S}_{nm}$  are known till degree and order  $N_{\max}$ , one can compute  $f(\theta_i, \lambda_j)$  as follows:

$$\tilde{f}(\theta_i, \lambda_j) = \sum_{n=0}^{N_{\max}} \sum_{m=0}^n (\bar{C}_{nm} \cos m\lambda_j + \bar{S}_{nm} \sin m\lambda_j) \bar{P}_{nm}(\cos \theta_i),\tag{20}$$

which can be regarded as an approximation to  $f(\theta, \lambda)$  at point  $(\theta_i, \lambda_j)$ . Expression (20) defines the object of spherical harmonic synthesis: given the coefficients, it is required to estimate the function.

The double summation appearing in (19) for harmonic analysis as well as in (20) for spherical harmonic synthesis are computed using FFT. Colombo (1981) has written two subroutines for this purpose, called HARMIN and SSYNTH, if the field is known on the surface of the sphere. Abd-Elmotaal (2004) has introduced an algorithm, using FFT technique, to allow the harmonic analysis and synthesis if the field is known on the surface of the ellipsoid using an iterative process to obtain the best coefficients accuracy as well as the minimum residual field.

#### 5.4. Tailored Geopotential Model for Egypt

The merged  $30' \times 30'$  global field has been used to estimate the harmonic coefficients of the tailored reference model by HRCOFITR program (Abd-Elmotaal, 2004) till degree and order 360. The higher harmonics (from  $n = 361$  to  $n = 2160$ ) of the EGM2008 global geopotential model have been restored to generate the ultra high-degree tailored geopotential model for Egypt complete to degree and order 2160. This tailored model will be called in the sequel EGTGM2014.

Figure 9 shows the lower harmonics (till  $n = 360$ ) of the EGTGM2014 tailored geopotential model for Egypt with comparison to EGM2008 global geopotential model.

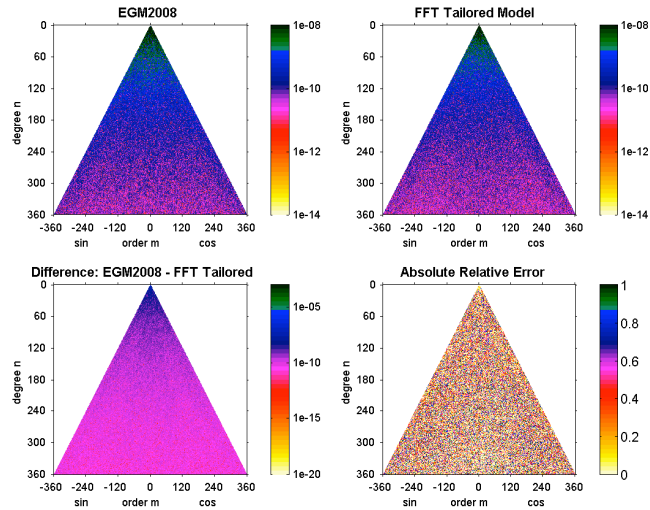


Figure 9: The lower harmonics (till  $n = 360$ ) of the EGTGM2014 tailored geopotential model for Egypt.

Figure 10 shows the differences at the grid points between the Egyptian  $30' \times 30'$  interpolated gravity anomalies and the estimated gravity anomalies using the EGTGM2014 ultra high-degree tailored geopotential model for Egypt. These differences measure the accuracy of the EGTGM2014 tailored geopotential model at the grid points. These differences range between  $-32.37$  mgal and  $27.59$  mgal with an average of about zero and a standard deviation of  $5.12$  mgal. The white areas in Fig. 10 indicate differences less than  $5$  mgal in magnitude, which shows a great matching over the Egyptian territory.

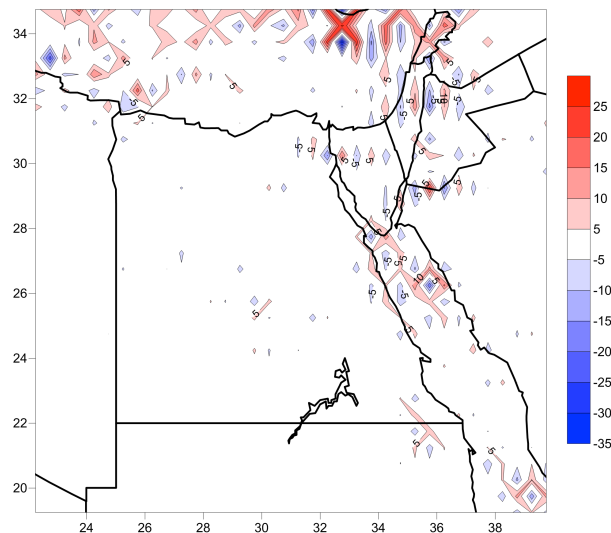


Figure 10: Differences between the Egyptian  $30' \times 30'$  interpolated gravity anomalies and the computed gravity anomalies using the EGTGM2014 tailored geopotential model.

Values are in mgal.

## 6. GRAVITY REDUCTION

The geoid computation in this investigation is carried out using the window remove-restore technique. The reduction step has been performed using (15). The contribution of the geopotential models to the gravity anomalies have been computed using the fast algorithm described in (Abd-Elmotaal, 1998). Alternative techniques are available in, e.g., (Rapp, 1982; Tscherning et al., 1994).

For the terrain reduction  $\Delta g_{TC\ win}$ , the topography and its compensation for the whole fixed data window ( $19^\circ N \leq \phi \leq 35^\circ N; 22^\circ E \leq \lambda \leq 40^\circ E$ ) have been considered. A constant value for the density of the topography of  $2.67 \text{ g/cm}^3$  is used. A value of  $0.4 \text{ g/cm}^3$  is used for the density contrast between the crust and mantle and a normal crustal thickness of 30 km has been used. The computation of the terrain reduction has been carried out using TC program, written originally by Forsberg (1984) after **major modifications** by Abd-Elmotaal and Kühtreiber (2003).

Table 2 illustrates the statistics of the free-air and Airy window isostatic anomalies using both EGM2008 and EGTGM2014 geopotential models complete to degree and order 2160. It shows that using the EGTGM2014 tailored geopotential model gives the best reduced anomalies. The variance has dropped by about 35% compared to that when using the window technique with EGM2008 geopotential model. Figure 11 illustrates the Airy window isostatic anomalies using the EGTGM2014 tailored geopotential model. It shows that the anomalies hardly exceed 20 mgal in magnitude over the Egyptian territory.

Finally, the reduced gravity anomalies are gridded on a  $30' \times 30'$  geographical grid using kriging interpolation technique. This step is needed for the geoid computation using the FFT technique.

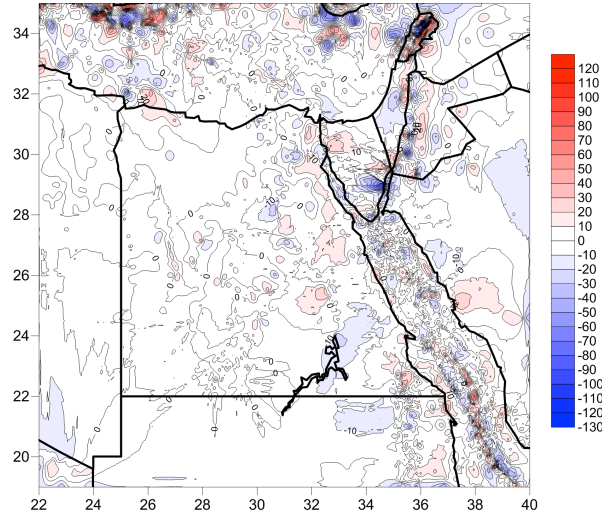


Figure 11: Airy window isostatic anomalies for Egypt using the EGTGM2014 tailored geopotential model. Contour interval: 10 mgal.

Table 2: Statistics of the gravity anomalies in Egypt (102418 gravity stations)

gravity anomalies	statistical parameters				
	min.	max.	average	st. dev.	variance
	mgal	mgal	mgal	mgal	mgal <sup>2</sup>
Free-air	-210.60	314.99	-27.58	50.65	2565.1
Airy Window (EGM2008)	-99.15	122.49	-0.26	20.46	418.6
Airy Window (EGTGM2014)	-134.30	112.69	-0.45	16.45	270.5

## 7. STOKES' INTEGRAL WITH 1D-FFT TECHNIQUE

The geoid undulation  $N$  can be calculated from the gridded gravity anomalies by using the well known Stokes' integral (Heiskanen and Moritz, 1967, p. 94)

$$N = \frac{R}{4\pi\gamma} \iint_{\sigma} \Delta g S(\psi) d\sigma, \quad (21)$$

where  $\gamma$  is the normal gravity,  $R$  is the mean earth's radius and  $S(\psi)$  stands for the Stokes function given by (ibid., p. 94)

$$S(\psi) = \frac{1}{s} - 4 - 6s + 10s^2 - (3 - 6s^2) \ln(s + s^2) \quad (22)$$

with

$$s = \sin \frac{\psi}{2}, \quad (23)$$

and  $\psi$  is the spherical distance between the computational point  $P$  and the running point  $Q$ , given by (Strang van Hees, 1990, p. 236)

$$\sin^2 \frac{1}{2} \psi_{PQ} = \sin^2 \frac{1}{2} (\phi_P - \phi_Q) + \sin^2 \frac{1}{2} (\lambda_P - \lambda_Q) \cos \phi_P \cos \phi_Q. \quad (24)$$

For discrete integration the area is divided into blocks of equal  $\Delta\phi$  and  $\Delta\lambda$ , so that the Stokes integral (21) can be replaced by the summation

$$N(\phi_P, \lambda_P) = \frac{R \Delta\phi \Delta\lambda}{4\pi\gamma} \sum_Q (\Delta g_Q \cos \phi_Q) S(\psi_{PQ}). \quad (25)$$

The Stokes integral (25) may be written as:

$$N_{\phi_P}(\lambda) = \frac{R \Delta\phi \Delta\lambda}{4\pi\gamma} \sum_{\phi_Q} \cos \phi_Q \sum_{\lambda_Q} \Delta g_Q S(\psi_{PQ}), \quad (26)$$

where  $N_{\phi_P}(\lambda)$  stands for the geoid undulation at all points on the same parallel of latitude  $\phi_P$ . The Stokes' kernel function  $S(\psi_{PQ})$  in the inner summation over  $\lambda_Q$  in (26) depends only on  $(\lambda_P - \lambda_Q)$ ,  $\phi_P$  and  $\phi_Q$  (see (24)), which can be written as:

$$S(\psi_{PQ}) = S_{\phi_P \phi_Q}(\lambda_P - \lambda_Q) = S_{\phi}(\lambda_P - \lambda_Q). \quad (27)$$

Hence (26) can be re-written as:

$$N_{\phi_P}(\lambda) = \frac{R \Delta\phi \Delta\lambda}{4\pi\gamma} \sum_{\phi_Q} \cos \phi_Q \sum_{\lambda_Q} \Delta g_Q S_{\phi}(\lambda_P - \lambda_Q). \quad (28)$$

The inner summation over  $\lambda_Q$  in (28) represents a one-dimensional convolution integral in the longitude direction since  $\phi_P$  and  $\phi_Q$  are constants within the summation. Hence, it can be evaluated by means of FFT technique. Thus  $N_{\phi_P}(\lambda)$  can be given by (Haagmans et al., 1993)

$$N_{\phi_P}(\lambda) = \frac{R \Delta\phi \Delta\lambda}{4\pi\gamma} \sum_{\phi_Q} \cos \phi_Q \left[ \sum_{\lambda_Q} \Delta g_Q \cos \phi_Q \right]^{-1} [S_{\phi}(\lambda_P - \lambda_Q)], \quad (29)$$

where  $\sum_1$  and  $\sum_1^{-1}$  stand for the one-dimensional Fourier transform and its inverse, respectively. Equation (29) is repeated for all parallel of latitudes for the area of interest.

## 8. GEOID COMPUTATION

The restore step of the window remove-restore technique (4) can be written in detail as

$$N = N_{GM_T} \Big|_{0 \leq n \leq 360} + N_{GM} \Big|_{361 \leq n \leq 2160} - N_h + N_{\Delta g} + N_{TC \text{ win}}, \quad (30)$$

where  $N_h$  stands for the contribution of the harmonic coefficients, computed using (8), of the topographic-isostatic masses of the data window. All other terms have been defined in sec. 3.

The contribution of the gravity anomalies to the geoid undulation  $N_{Ag}$  has been computed by the 1D-FFT technique (29) using the FFTGEOID program by (Sideris and Li, 1993). The contribution of the topography and its compensation  $N_{TC\ win}$  has been computed using the modified TC program (Abd-Elmotaal and Kühtreiber, 2003). Both the EGM2008 and the tailored EGTGM2014 global geopotential models complete to degree and order 2160 have been used to compute the contribution of the reference field on the geoid undulations. The EGH13M03 30'  $\times$  30' DHM (Abd-Elmotaal and Ashry, 2013) has been used to compute the harmonic coefficients, using (8), needed for the computation of the topographic-isostatic masses of the data window on the geoid undulation  $N_h$ .

Figure 12 shows the difference between the geoid computed by using the EGM2008 geopotential model within the window remove-restore technique with Airy-Heiskanen isostatic model  $N_{Airy\ win\ EGM\ 2008}$  and the geoid derived from the combination of the GPS and leveling  $N_{GPS}$ . The difference, before removing the trend, ranges from  $-10.65$  m to  $3.78$  m with an average of  $-1.20$  m and a standard deviation of  $3.00$  m. The structure of the differences shows non-linear long-wavelength behaviour with a high east-west gradient.

Figure 13 shows the difference between the geoid computed by using the EGTGM2014 tailored geopotential model within the window remove-restore technique with AiryHeiskanen isostatic model  $N_{Airy\ win\ EGTGM\ 2014}$  and  $N_{GPS}$ . The difference, before removing the trend, ranges from  $0.80$  m to  $10.24$  m with an average of  $5.44$  m and a standard deviation of  $2.33$  m. Figure 13 shows also non-linear long-wavelength behaviour of the differences but with much less range and gradient. The range and standard deviation have dropped by about 35% and 22%, respectively, compared to those when using the window technique with EGM2008 geopotential model.

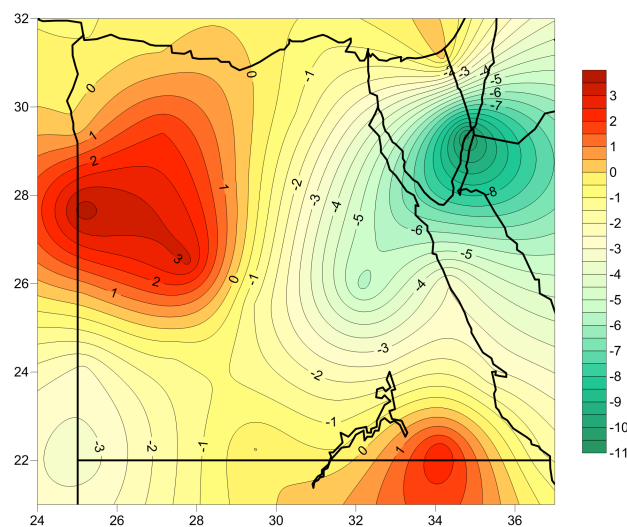


Figure 12: Geoid difference ( $N_{GPS} - N_{Airy\ win\ EGM\ 2008}$ ) for Egypt. Contour interval: 0.5 m.

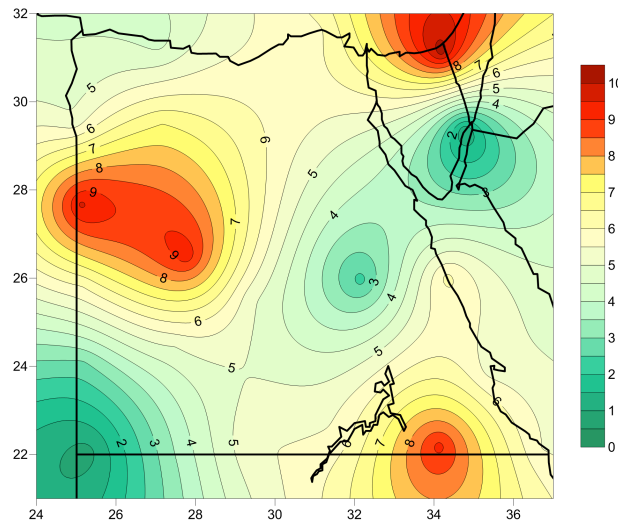


Figure 13: Geoid difference ( $N_{GPS} - N_{Airy\ win\ EGTGM\ 2014}$ ) for Egypt. Contour interval: 0.5 m.

The computed geoids have been fitted to the GPS/levelling derived geoid by removing a trend surface. A kriging trend function has been computed using only 27 GPS stations among the available 30 GPS stations in Egypt (cf. Fig. 3). Table 3 shows the statistics of the remaining differences after removing a kriging trend function at the 27 GPS stations used for the geoid fitting. This represents an internal check of the quality of the computed geoid. Table 3 shows that the range of the remaining differences after removing the trend function is smaller by about 10% when using the EGTGM2014 tailored geopotential model.

Table 4 shows that statistics of the remaining differences after removing a kriging trend function at the 3 GPS stations which were not used for the geoid fitting. This represents an external check of the quality of the computed geoid. Table 4 shows that using the EGTGM2014 tailored geopotential model improves the external geoid accuracy by about 20%, and the range of the remaining differences has dropped by about 22 %.

Table 3: Statistics of the remaining differences at the 27 GPS stations used for the geoid fitting after removing a kriging trend function

geoid type	statistical parameters			
	min.	max.	average	st. dev.
	cm	cm	cm	cm
$N_{Airy\ win\ EGM\ 2008}$	-9.2	9.8	0.2	3.4
$N_{Airy\ win\ EGTGM\ 2014}$	-7.6	9.8	0.2	3.3

It should be noted that the external geoid accuracy can hardly be estimated by only 3 GPS stations. The values here are only for comparison purpose. It is, however, believed that the actual accuracy of the computed geoid is far better, but this needs more GPS stations to fairly judge the geoid external accuracy.

Table 4: Statistics of the remaining differences after removing a kriging trend function at the 3 GPS stations which were not used for the geoid fitting

geoid type	statistical parameters			
	min.	max.	average	st. dev.
	m	m	m	m
$N_{Airy\ win\ EGM\ 2008}$	-1.40	2.46	0.29	1.97
$N_{Airy\ win\ EGTGM\ 2014}$	-0.88	2.13	0.30	1.60

Finally, Fig. 14 shows the gravimetric geoid for Egypt using the tailored EGTGM08 geopotential model in the framework of the window remove-restore technique fitted to 27 GPS stations using the kriging trend function. The values of the geoid range between 5.50 m and 23.69 m with an average of 14.41 m and standard deviation of 3.78 m.

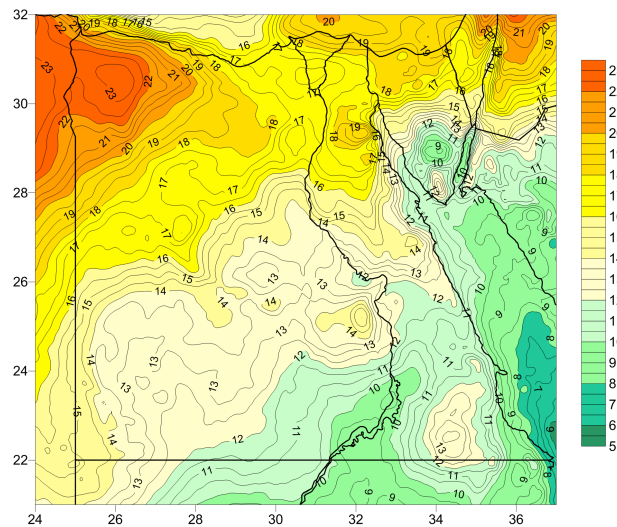


Figure 14: Gravimetric geoid for Egypt using the tailored EGTGM2014 geopotential model with window technique fitted to 27 GPS stations using the kriging trend function. Contour interval: 0.5 m.

## 9. CONCLUSIONS

An ultra high-degree tailored reference geopotential model for Egypt, complete to degree and order 2160, has been developed in this investigation. An FFT technique using an iterative process has been used to estimate the harmonic coefficients to enhance the accuracy of the obtained harmonic coefficients and to minimize the residual field. The window remove-restore technique has been applied to get rid of the double consideration of the topographic-isostatic masses within the data window. The tailored geopotential model created in this investigation gives better residual gravity anomalies (unbiased and have much less variance). The variance has dropped by about 35 %.

Gravimetric geoids for Egypt have been computed in this investigation using both the EGM2008 and the EGTGM2014 tailored geopotential models in the framework of the window remove-restore technique using the 1D-FFT technique. The computations were based on all currently available land and sea free-air gravity anomaly data. The computed geoids have been fitted to the GPS/levelling derived geoid by removing a trend surface. A kriging trend function has been computed using only 27 GPS stations among the available 30 GPS stations in Egypt (cf. Fig. 3). The internal precision of the fitted geoids is very good (about 3 cm) and it is nearly equal for both geoids. Using the EGTGM2014 tailored geopotential model improves the external geoid accuracy by about 20%, and the range of the remaining differences has dropped by about 22 %.

Finally, it should be noted that the distribution of the GPS stations in Egypt is fairly good; however, the number of the GPS stations should be significantly increased for better geoid fitting. **In addition, the poor gravity coverage in Egypt is remarkable. An airborne gravity survey may suggest itself to greatly improve the gravity coverage over Egypt.**

## REFERENCES

- Abd-Elmotaal, H. (1998) An Alternative Capable Technique for the Evaluation of Geopotential from Spherical Harmonic Expansions, *Bollettino di Geodesia e Scienze Affini*, **57**, 25–38.
- Abd-Elmotaal, H. (2004) An Efficient Technique for Harmonic Analysis on a Spheroid (Ellipsoid and Sphere), *Österreichische Zeitschrift für Vermessung & Geoinformation*, **3+4**, 126–135.
- Abd-Elmotaal, H. (2007) Reference Geopotential Models Tailored to the Egyptian Gravity Field, *Bollettino di Geodesia e Scienze Affini*, **66** (3), 129–144.
- Abd-Elmotaal, H. (2009) Evaluation of the EGM2008 Geopotential Model for Egypt. *Newton's Bulletin*, **4**, 185–199.**
- Abd-Elmotaal, H. and Ashry, M. (2013) The 3" Digital Height Model for Egypt – EGH13, 8th International Conference of Applied Geophysics, Cairo, Egypt, February 25–26, 2013.
- Abd-Elmotaal, H. and Kühtreiber, N. (2003) Geoid Determination Using Adapted Reference Field, Seismic Moho Depths and Variable Density Contrast, *Journal of Geodesy*, **77**, 77–85.

- Abd-Elmotaal, H., Seitz, K., Abd-Elbaky, M. and Heck, B. (2013) Tailored Reference Geopotential Model for Africa, Scientific Assembly of the International Association of Geodesy, Potsdam, Germany, September 1–6, 2013.
- Colombo, O. (1981) Numerical Methods for Harmonic Analysis on the Sphere, Department of Geodetic Science, The Ohio State University, Columbus, Ohio, **310**.
- Elliott, D., and Rao, K.R. (1982) Fast Transforms: Algorithms, Analysis, Applications. Academic Press.
- Farr, T.G., Rosen, P.A., Caro, E., Crippen, R., Duren, R., Hensley, S., Kobrick, M., Paller, M., Rodriguez, E., Roth, L., Seal, D., Shaffer, S., Shimada, J., Umland, J., Werner, M., Oskin, M., Burbank, D. and Alsdorf, D. (2007) The Shuttle Radar Topography Mission, *Reviews of Geophysics*, **45**, RG2004, DOI: 10.1029/2005RG000183.
- Forsberg, R. (1984) A Study of Terrain Reductions, Density Anomalies and Geophysical Inversion Methods in Gravity Field Modelling, Department of Geodetic Science, The Ohio State University, Columbus, Ohio, **355**.
- Haagmans, R., de Min, E. and van Gelderen, M. (1993) Fast Evaluation of Convolution Integrals on the Sphere Using 1D FFT, and a Comparison with Existing Methods for Stokes' Integral, *manuscripta geodaetica*, **18**, 227–241.
- Heiskanen, W.A., and Moritz, H. (1967) Physical Geodesy. Freeman, San Francisco.
- Kearsley, A.H.W., and Forsberg, R. (1990) Tailored Geopotential Models – Applications and Shortcomings, *manuscripta geodaetica*, **15**, 151–158.**
- Pavlis, N.K., Holmes, S.A., Kenyon, S.C., and Factor, J.K. (2008) An Earth Gravitational Model to Degree 2160: EGM2008, General Assembly of the European Geosciences Union, Vienna, Austria, April 13–18, 2008.
- Pavlis, N.K., Holmes S.A., Kenyon S.C., and Factor J.K. (2012) The development and evaluation of the Earth Gravitational Model 2008 (EGM2008). *Journal of Geophysical Research* **117**, B04406, DOI: 10.1029/2011JB008916.
- Rapp, R.H. (1982) A Fortran Program for the Computation of Gravimetric Quantities From High Degree Spherical Harmonic Expansions, Department of Geodetic Science, The Ohio State University, Columbus, Ohio, **334**.
- Rummel, R., Rapp, R.H., Sünkel, H., and Tscherning, C.C. (1988) Comparison of Global Topographic/Isostatic Models to the Earth's Observed Gravity Field, Department of Geodetic Science, The Ohio State University, Columbus, Ohio, **388**.
- Sideris, M.G. and Li, Y.C. (1993) Gravity Field Convolutions without Windowing and Edge-Effects, *Bulletin Géodésique*, **67**, 107–118.
- Strang van Hees, G. (1990) Stokes Formula Using Fast Fourier Techniques, *manuscripta geodaetica*, **15**, 235–239.
- Sünkel, H. (1985) An Isostatic Earth Model, Department of Geodetic Science, The Ohio State University, Columbus, Ohio, **367**.
- Tscherning, C.C., Knudsen, P. and Forsberg, R. (1994) Description of the GRAVSOF T Package, Geophysical Institute, University of Copenhagen, Technical Report.
- Wenzel, H.G. (1998) Ultra High Degree Geopotential Models GPM98A, B and C to Degree 1800 Tailored to Europe, *Reports of the Finnish Geodetic Institute*, **98** (4), 71–80.

## BIOGRAPHICAL NOTES

Prof. Dr. Hussein A. Abd-Elmotaal graduated in the Faculty of Engineering, Ain Shams University, Egypt in 1983. He has received his Ph.D. in geodesy at the Graz University of Technology, Austria, in 1991. He joined the staff of the Civil Engineering Department, Minia University since 1984. He is a professor of surveying and geodesy, Department of Civil Engineering, Minia University since 2002. He won the International Association of Geodesy (IAG) Best Paper Award in 1993. He has been awarded the State Prize in Engineering Sciences in 2003. He has received the Ideal Professor Prize for the Faculty of Engineering, Minia University in 2008. Prof. Abd-Elmotaal has been appointed IAG Fellow, 2011 in recognition of his esteemed services rendered to geodesy during the past 20 years. Prof. Hussein Abd-Elmotaal is the Chairman of the IAG Sub-Commission 2.4 “Regional Geoid Determination” (<http://www.iag-commission2.ch/steering.htm>) since 2011. He chairs the IAG Regional Sub-Commission “Gravity and Geoid in Africa” (<http://www.iag-commission2.ch/ToRSC.htm>) since 2007. Prof. Abd-Elmotaal has chaired the Department of Civil Engineering, Minia University from 2004 until 2007.

Prof. Abd-Elmotaal is an international reviewer for peer-reviewed international journals and projects since 1995. He is a member of the Egyptian National Examiners Committee for promoting university staff members (Surveying and Geodesy), since 2008. He is a member of the Egyptian National Committee for Geodesy and Geophysics, since 2007. He is a member of the Egyptian National Committee for Surveying and Mapping, since 2006. He has participated in more than 40 international conferences. He has more than 100 research publications in peer-reviewed international journals and conferences. Prof. Abd-Elmotaal is an Associate Editor of the Journal of the International Association of Geodesy Symposia.

## CONTACTS

Prof. Dr. Hussein A. Abd-Elmotaal  
Professor of Surveying and Geodesy  
Civil Engineering Department  
Faculty of Engineering  
Minia University  
Minia 61111  
EGYPT  
Tel: +20-86-2364510  
Fax: +20-86-2346674  
E-mail: [abdelmotaal@lycos.com](mailto:abdelmotaal@lycos.com)  
URL: <http://mu.minia.edu.eg/Geodesy/AFRgeo/hussein.htm>  
Google Scholar: <http://scholar.google.com/citations?user=1yCeSZwAAAAJ>